Journal of Alloys and Compounds, 197 (1993) 137–144
JALCOM 7305

First principles methods for structural trends in oxides: applications to crystalline silica

James R. Chelikowsky, Nadia Binggeli and Nitin R. Keskar
Department of Chemical Engineering and Materials Science, Minnesota Supercomputer Institute, University of Minnesota, Minneapolis, MN 55455 (USA)

Abstract

One goal of crystal chemistry is to construct approaches to compute from "first principles" the structural properties of ordered compounds. Such an approach is particularly valuable for families of structures with a given stoichiometry. An example of this case is crystalline silica. SiO_2 may exist in a variety of structures which are nearly identical in terms of binding energies. We will illustrate how first principles methods may be employed to predict the relative stability of silica polymorphs, and how these forms may transform under pressure to other ordered, or disordered, phases. Our methods are based on *ab initio* pseudopotentials constructed within the local density approximation. These pseudopotentials have been optimized for use with a plane wave basis and should be widely applicable for determining the crystal stability of silicates and related materials.

1. Introduction

Today it is possible to predict accurately the structural parameters of a crystal with the only input being the atomic species present. One of the first applications of total energy calculations was to consider the tetrahedral crystals of carbon, silicon and germanium [1]. The lattice parameters of these crystals were computed to within 1%–2%, and superconducting forms of silicon were predicted on the basis of these techniques [2]. In the past few years, these methods have been successfully applied to a variety of materials ranging from rare earths, to transition metals, to oxides [3]. Surfaces and interfaces, and properties of amorphous solids have also been considered [1]. Properties of small clusters have been computed with an accuracy rivalling sophisticated quantum chemistry techniques in terms of the bond lengths and angles, [4, 5]. Typically, the accuracy of these methods is a few per cent not only for bond lengths, but also for phonon energies and elastic constants. These methods may also be used to examine dynamical effects. Applications have been made to semiconducting systems, and the nucleation process in small silicon clusters [5]. There are no inherent limitations with respect to the size of the system for these methods, save computing power.

However, these methods are not particularly valuable for obtaining an "overview" of chemical trends for related crystalline families. The computations are simply too intensive, and a case by case study is a more appropriate mode. For example, to assess possible candidates for forming quasi-crystals [6], one might wish to consider several hundred candidate structures. In this case, chemical coordinates based on orbital radii, electronegativity and electron count are more useful. These coordinates can be used to systematize a large body of crystal structure data with literally thousands of entries. However, there are important applications for crystal trends which are not appropriate for chemical coordinates. For a fixed stoichiometry, it is not possible to use chemical coordinates to explore regularities in polymorphs. An example of this case is crystalline silica. SiO_2 may exist in a variety of structures which are nearly identical in terms of binding energies. In this paper, we will illustrate how first principles methods may be employed to predict accurately which forms of SiO_2 are most stable and how these forms may transform under pressure. We will also briefly discuss other issues which may be handled by "first principles" methods such as understanding the driving force for the amorphization of quartz under pressure.

2. Numerical methods

In this section, we review briefly the numerical methods employed to compute the total electronic energy of silica structures. We employ *ab initio* pseudopotentials [7] which are constructed within the local density approximation (LDA) [8–10]. The LDA is a powerful

0925-8388/93/$6.00

approximation which allows one to map the many-body problem onto a one-electron problem. Within this approximation, the total electronic potential for the valence electrons is written as

$$V_{\text{total}}(\boldsymbol{r}) = V_{\text{ion}}(\boldsymbol{r}) + V_{\text{H}}(\boldsymbol{r}) + V_{\text{xc}}[\rho(\boldsymbol{r})] \quad (1)$$

V_{ion} corresponds to the interaction potential between the valence electrons, and the nucleus and tightly bound core electrons, *i.e.* the ion-core pseudopotential. V_{H} corresponds to the electrostatic interactions between the valence electrons and V_{xc} corresponds to the effective exchange-correlation potential between the valence electrons. This latter term is the basis of the LDA; the exchange-correlation potential at a point $\boldsymbol{r}$ depends only on the electron density $\rho(\boldsymbol{r})$ at that point.

The replacement of the all electron potential with a pseudopotential has a number of advantages when compared with an all electron calculation. Core states are not considered, and only the properties of the chemically active valence states are reproduced. In the case of silica, the $1s^2$, $2s^2$, $2p^6$ states in silicon are treated as chemically inert, as is the $1s^2$ state in oxygen. Since only the valence states are replicated by the pseudopotentials, simple bases can be used. One of the most useful bases is a basis composed of plane waves. The advantages of a plane-wave basis are numerous: the basis is complete, no shape approximations are made, the set is orthogonal/orthonormal, and the electrostatic potential can be evaluated trivially with a plane wave basis.

Our pseudopotentials were generated using the method of Troullier and Martins [3]. Their method produces "soft" pseudopotentials, *i.e.* pseudopotentials which allow a rapid convergence in terms of a plane wave basis. The oxygen ion core pseudopotential was generated from the atomic $2s^22p^4$ ground state configuration with a radial cut-off of 1.45 a.u. The pseudo-wavefunctions converge to the "all electron" wavefunctions outside of this cut-off; within the cut-off the pseudo-wavefunctions are nodeless. The oxygen pseudopotential was not adjusted to replicate the unoccupied 3d-states as these states are not expected to contribute significantly to the chemical bond. For silicon, s-, p-, and d-components of the potential were included. The radial cut-off for all three components was taken to be 1.80 a.u.

Given an ion core pseudopotential, the valence electrons are allowed to respond to the potentials to form a self-consistent total potential. Initially, an approximate potential is used to solve the one-electron Schrödinger equation. The wavefunctions from the solution of this approximate potential are then used to construct a new potential which in turn can generate new wavefunctions from which the potential can be updated again. When the "input" potential agrees with the "output" potential, a self-consistent field has been obtained.

The one-electron Schrödinger equation for a periodic crystal has the form:

$$\left[\frac{-\hbar^2\nabla^2}{2m} + V_{\text{ion}} + V_{\text{H}} + V_{\text{xc}}\right]\psi_{\text{n},\boldsymbol{k}}(\boldsymbol{r}) = E_{\text{n}}(\boldsymbol{k})\psi_{\text{n},\boldsymbol{k}}(\boldsymbol{r}) \quad (2)$$

This equation was solved using a fast iterative diagonalization method [11, 12]. One advantage of this method is that it does not require a calculation of the full hamiltonian matrix. Rather, only $H\psi$ is calculated. This procedure leads to a dramatic reduction in storage, and a considerable reduction in computing time. Plane waves up to an energy cut-off of 64 Ry were included in the basis. Even for a relatively simple form of crystalline silica, such as α-quartz, this entails a few thousand plane waves in the basis. We have increased the cut-off to 144 Ry and estimate the total energy to be converged to within 0.01 eV per molecular unit for the crystalline forms of SiO_2 examined here.

Once the Schrödinger equation is solved, the energy and spatial distributions of the valence electrons are known [13]. The total electronic energy can be obtained from terms of the form:

$$E_{\text{total}} = E_{\text{core-core}} + [E_{\text{kinetic}} + E_{\text{core-electron}} + E_{\text{electron-electron}}] \quad (3)$$

The first term corresponds to the Coulomb interactions of the ion cores. Since the cores are treated as rigid, this term can be evaluated by a Ewald summation. The remaining terms are evaluated using the electronic pseudo-wavefunctions. The kinetic energy E_{kinetic} is evaluated trivially in a plane wave basis. The ion core–electron term $E_{\text{core-electron}}$ is evaluated from the valence charge density and a knowledge of the ion core pseudopotential. The most complicated term is the electron–electron term $E_{\text{electron-electron}}$. This term contains Coulomb terms from the Hartree potential V_{H} which must be included in a Ewald summation with the core–core interactions. The energy of this term corresponds to each valence electron moving in an average potential generated by the other electrons. The term also includes exchange-correlation energies resulting from V_{xc}. Within the local density approximation, these terms can be evaluated once a self-consistent charge density has been constructed.

The goal of a total energy calculation is to determine the total electronic energy for a given structure, or structures. For example, we might consider a number of candidate structures for SiO_2. Since crystalline silica often condenses in complex structures with a number of internal parameters, it is non-trivial to evaluate the structural energy. For example, the α-quartz structure has three molecular units in the hexagonal unit cell. The cell shape is determined by the c/a ratio, and four

internal parameters fix the positions of the silicon and oxygen atoms within the cell [14]. At each volume, the shape and internal structure of the crystal must be optimized by minimizing the total energy. It is possible to expedite this procedure by calculating the forces on each atom using the Hellman–Feynman theorem [15]. The atoms can then be moved according to the computed forces to minimize the structural energy. One can use the energy *vs.* volume calculations to determine the enthalpy of the structure as a function of volume, or pressure. This type of calculation can be used to predict which phase of silica will be most stable as a function of pressure. Moreover, the results can be used to predict such ground state properties as the cohesive energy, ambient structural parameters, and bulk moduli of virtually any crystalline form of silica [15–18].

The chief limitation of this procedure resides in the local density approximation. This approximation generally gives structural properties to within approximately 1%–2%. The cohesive energies are not determined so accurately, and the binding energy is usually overestimated by 5%–10%. However, the relative energy differences between solid state structures are more accurately calculated. Structural energy differences as small as approximately 0.01 eV per atom can be reliably predicted within the LDA. Another issue which limits the applicability of these methods centers on computational limitations. At present, we can routinely handle unit cells with no more than 10–15 molecular units of SiO_2 using supercomputers.

While the calculations we present here omit the role of temperature, it is possible to include the temperature dependence of the structural properties. For example, one can include phonon contributions to entropy and construct a free energy. However, if one is interested in similar structures, the inclusion of temperature may not be so important. The errors introduced by the LDA may be greater than the effect of temperature on a given structure.

3. Structure of crystalline silica

Broadly speaking, crystalline silica may be classified by the coordination of the silicon cation. In the most stable forms of crystalline silica, silicon is four-fold coordinated and the structures may be thought to consist of $Si(O_4)_{1/2}$ tetrahedral units. Within these units, the O–Si–O bond angles are close to the ideal tetrahedral angle of 109.5°. The tetrahedral units are linked via bridging oxygen atoms. The Si–O–Si bond angles center near about 140° with a range of $\pm 20°$. These bridging oxygen bond angles are quite pliant and the differences between four-fold coordinated crystals of SiO_2 can be traced to how the tetrahedral units are linked together.

When subjected to pressure, one might expect the coordination of the cations, and anions, in a crystalline phase to increase. In the case of silica, this has been an area of some conjecture. Over 30 years ago, a new phase of SiO_2 in the rutile structure was discovered, *i.e.* stishovite. Stishovite can be formed from silica under pressure, yet it can exist in a metastable state under ambient conditions. In this form of crystalline silica, silicon is six-fold coordinated. Questions as to the denser forms of silica beyond stishovite have been raised in the context of mineral physics.

In Fig. 1, we illustrate some of the common forms of crystalline silica along with possible high pressure forms. The structures with SiO_2 tetrahedral units include α- and β-quartz. Known dense phases of silica include stishovite which corresponds to the rutile structure. Possible high density phases of silica include fluorite, and a distortion of the fluorite structure, the $Pa\bar{3}$ structure. In particular, it might seem that a "fluorite-like" structure would be an appropriate candidate for a high pressure form of silica as the cation in such a structure is eight-fold coordinated.

In Fig. 2, we illustrate the energy of the structures as a function of volume. These curves were generated by fitting a standard equation of state such as the Birch equation [19] to computed energies as a function of volume. Consistent with experiment, we find that the lowest energy phase is the α-quartz structure which is a distortion of the β-quartz structure. The stishovite structure is nearly as stable as the quartz structure, but the equilibrium molecular volume is considerably

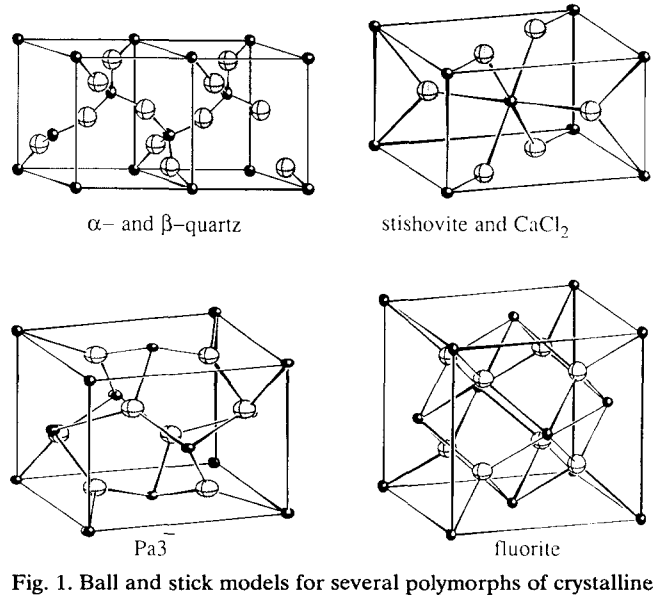

Fig. 1. Ball and stick models for several polymorphs of crystalline silica. α- and β-quartz possess four-fold silicon cations. The stishovite and the $CaCl_2$ structures possess six-fold cations. Proposed high pressure forms of crystalline silica include the $Pa\bar{3}$ structure and the fluorite structure. These latter structures possess eight-fold coordinated cations.

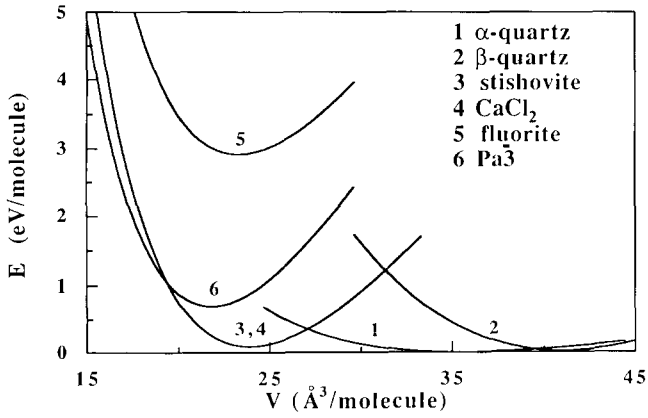

Fig. 2. Equations of state for several polymorphs of silica. The curves were generated by fitting a Birch equation of state [19] to the theoretical calculations.

smaller owing to the higher coordination in the stishovite structure. The $CaCl_2$ structure, which corresponds to a distorted stishovite structure [18, 20], is nearly degenerate in energy with stishovite in our calculations.

Perhaps the most interesting aspect of Fig. 2 is the prediction that the $Pa\bar{3}$ structure should be stable under high pressure whereas the fluorite structure is not. Our calculations predict that the density of the fluorite is slightly lower than the density of the $Pa\bar{3}$ or the stishovite structures. From thermodynamics, it is not possible to convert a dense structure into a less dense structure with the application of isotropic pressure. The inclusion of temperature is unlikely to alter our calculations and this conclusion. Despite theoretical predictions indicating the high pressure stability of the $Pa\bar{3}$ structure, it has not been observed at pressures up to about 100 GPa. There may be kinetic barriers which inhibit the transformation of the stishovite, or $CaCl_2$, structure to the $Pa\bar{3}$ structure.

In Table 1, we list the calculated structural parameters which enter the Birch equations of state. The equation of state parameters include the equilibrium energy and volume, the bulk modulus, and pressure derivative of the bulk modulus. We have taken the equilibrium energy of α-quartz as the zero of energy. Relative to isolated pseudo-atoms of silicon and oxygen, we find quartz is over bound by about 15% *i.e.* we find the cohesive energy of quartz to be approximately 22.2 eV per molecular unit as compared with an experimental value of 19.2 eV per molecular unit. This is expected to be the case for an LDA calculation. The relative energies of the silica phases to α-quartz should be much more accurate. As expected, owing to the small structural differences, the energy difference between α- and β-quartz is only about 0.02 eV per molecular unit. Such a small energy difference is at the limit of accuracy of our methods. Stishovite is slightly higher in energy than α-quartz. This small energy difference is consistent with the observation that stishovite can coexist as a metastable phase with quartz. One might expect that if we were to include entropy in our calculation, the open quartz structure would be further stabilized *vs.* the stishovite structure. Open phases tend to have large phonon contributions to entropy when compared with dense phases. However, calorimetry measurements have indicated that the differences in the entropy between α-quartz and stishovite are smaller than one might have anticipated on the basis of this argument.

The equilibrium volumes for the five phases in Table 1 are in good agreement with experiment. The largest error is about 3%. Also, the bulk moduli are in good accord with experiment, except possibly for β-quartz. The experimental value [21] tabulated was taken at a high temperature, *i.e.* 873 K, and it is questionable whether this value can be compared with the theoretical value. We have tabulated the pressure derivatives of the bulk modulus and compared them with experiment. This quantity is difficult to determine experimentally, and the comparison is qualitative at best.

Ambient structural parameters from our calculations are listed in Table 2. The parameters are within a few per cent of experimental values. In both α- and β-quartz, the c-axis tends to be slightly larger than experiment. It is not clear whether this is a result of the LDA, or perhaps a technical issue associated with the asymmetry of the unit cell.

TABLE 1. Parameters of the Birch equation of state; α-quartz is taken to be the energy reference

Silica	Equilibrium energy (eV per molecule)	V_0 (Å³ per molecule)		B_0 (GPa)		B_0'	
		Experiment	Theory	Experiment	Theory	Experiment	Theory
α-quartz [21, 22]	0	37.710	37.86	37.1	38.1	6.0	3.90
β-quartz [13, 23]	0.017	39.634	41.05	56.4	135.1	–	1.91
Stishovite [24, 25]	0.086	23.308	22.82	313.0	292.0	6.0	5.86
Fluorite	2.914	–	23.29	–	300.1	–	4.13
$Pa\bar{3}$	0.699	–	21.82	–	347.0	–	3.89

TABLE 2. Structural parameters of silica polymorphs; the theoretical results are obtained using pseudopotentials; the experimental references are as in Table 1

Silica	Symmetry	Lattice constants (Å)		Internal coordinates	
		Experiment	Theory	Experiment	Theory
α-quartz	Hexagonal ($P3_121$)	$a=4.9160$ $c=5.4054$	4.89 5.49	$u=0.4697$ $x=0.4135$ $y=0.2669$ $z=0.1191$	0.469 0.418 0.274 0.118
β-quartz	Hexagonal ($P6_222$)	$a=5.01$ $c=5.47$	5.03 5.62	$u=0.197$	0.211
Stishovite	Tetragonal ($P4_2/mnm$)	$a=4.1801$ $c=2.6678$	4.14 2.67	$u=0.3062$	0.305
Fluorite	Cubic ($Fm\bar{3}m$)	–	$a=4.53$	–	–
$Pa\bar{3}$	Cubic ($Pa\bar{3}$)	–	$a=4.43$	–	$u=0.344$

4. Order–disorder transformations in silica

Another area where first principles calculations can be of great utility concerns the solid-state order–disorder transformation. Such transformations can be induced by pressure. At high pressures, α-quartz subsists as a metastable phase which gradually transforms to an amorphous form and, subsequently, to a rutile-like crystalline structure. Evidence for the onset of amorphization has been reported at about 15 GPa from single-crystal analysis [26]. In powder measurements [27], the transition is observed to be complete by about 35 GPa. Experiments performed on powdered samples at pressures above 60 GPa indicate a crystalline structure which is thought to resemble the stishovite structure [28].

One advantage of first principles structural energy calculations is that one can examine the theoretical evolution of the α-quartz crystalline phase at pressures above the amorphization transformation. It has been proposed that α-quartz would evolve under pressure to a structure in which the oxygen anions are arranged in a b.c.c. stacking, were it not for the fact that the crystal first amorphizes. The b.c.c. arrangement of oxygen anions was proposed [29] by an extrapolation of the trends observed during the compression of α-quartz and its low pressure isomorphic counterpart α-GeO_2.

We have tested this hypothesis by examining the arrangement of oxygen anions in α-quartz as a function of pressure [30]. At fairly high pressures, *e.g.* above about 50 GPa, we find that the anions are clearly tending toward a b.c.c. arrangement. For an ideal b.c.c. arrangement of oxygen anions, $x=y=1/3$ and $z=1/12$ in the Wyckoff notation [14] and the lattice ratio $c/a=(3/2)^{1/2}\approx 1.225$. Assuming ideally centered $Si(O_4)_{1/2}$ tetrahedra, we have $u=5/12\approx 0.417$ where u determines the position of the silicon cation. At ambient pressure, these parameters are $x=0.418$, $y=0.274$, $z=0.118$, $u=0.469$ and $c/a=1.125$. At a pressure near about 50 GPa, we find from our total energy calculations, $x=0.350$, $y=0.339$, $z=0.077$, $u=0.406$ and $c/a=1.149$. The total energy calculations confirm a pressure-induced tendency of the oxygen anions toward the b.c.c. structure, although the b.c.c. arrangement is not ideal as the c/a ratio is smaller than expected. In Fig. 3, we illustrate the b.c.c. arrangement of oxygen anions at high pressure in the α-quartz structure.

The b.c.c. packing is achieved at pressures significantly larger than the amorphization pressure. However, the main features associated with the b.c.c. packing already occur at pressures of the order of about 30 GPa. Oxygen b.c.c. packing, even in a non-ideal form, may promote the diffusion of the silicon cations. The body-centered

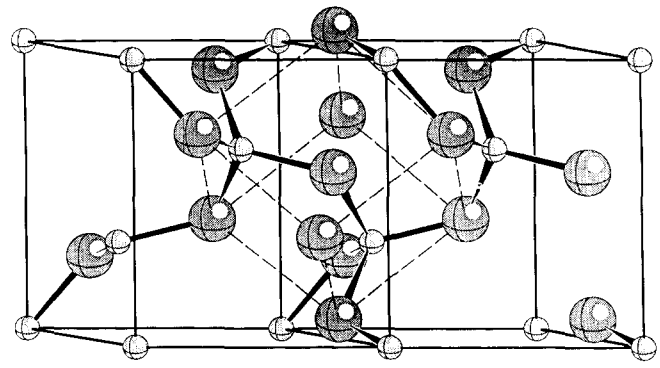

Fig. 3. Theoretical high pressure form for the α-quartz structure. The silicon cations are shown by the small spheres, oxygen anions by the large spheres. Note how the oxygen anions form a b.c.c. packing at high pressures.

cell has 12 equivalent tetrahedral sites and six octahedral sites. Only one of the tetrahedral sites is occupied in the α-quartz structure. Diffusion of silicon between the tetrahedral sites, or to a nearby octahedral site along "tunnels" formed by the columns of oxygen anions, may be a key process in the transformation to the amorphous state and the further transformation to the crystalline silicon six-fold coordinated structure. In Fig. 4, we note that one of the independent O–Si–O angles, which is equal to approximately 110° in α-quartz, increases to approximately 127° in the b.c.c. environment. This angle opening may provide a pathway for enhanced diffusion of the silicon cations from the four-fold to six-fold sites.

A closely related issue to the formation of the b.c.c. oxygen anion packing concerns the mechanical stability of α-quartz under pressure. It has been suggested that such an instability could drive the amorphization process [27, 31]. For example, b.c.c. packing could be inherently unstable against a shear. First principles calculations allow one to test such a hypothesis. We can understand, at least qualitatively, strain-induced non-linearities in α-quartz by examining changes in the bond angles with pressure. In Fig. 5, we plot the Si–O–Si and O–Si–O bond angles as a function of pressure. Except at very elevated pressures, the O–Si–O bonds remain near the tetrahedral angle of 109.5°. However, the Si–O–Si bridging bond angle is quite pliant. This angle is equal to 145° at ambient pressure; at around 20 GPa it is reduced to 125°. From roughly ambient pressures to 15 GPa, this angle varies linearly with pressure. Above 15 GPa, the angle exhibits a non-linear behavior with pressure. This non-linearity is indicative of a strained bond angle. Such a conclusion is consistent with quantum chemistry calculations on molecular fragments. These calculations

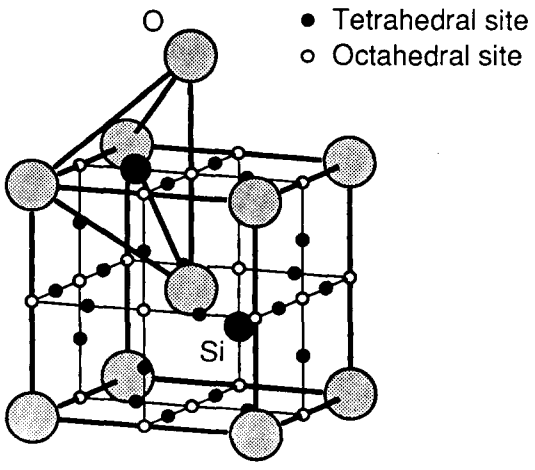

Fig. 4. Possible sites for silicon cations in a high pressure form of α-quartz. The b.c.c. packing of the oxygen anions may allow the "easy" diffusion of silicon cations from the tetrahedral sites to octahedral sites. Silicon cations in the octahedral sites share with stishovite a similar nearest-neighbor environment.

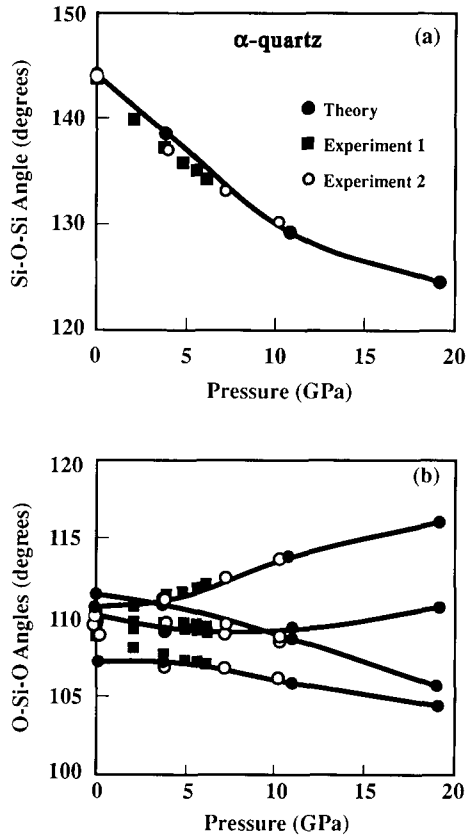

Fig. 5. Bond angles in α-quartz as a function of pressure. Above about 15 GPa, the bond angles behave in a non-linear manner, indicating the existence of a large internal strain energy. Experiment 1 is from ref. 22, experiment 2 is from ref. 15.

suggest that Si–O–Si angles below about 120° are very unfavorable in terms of generating a large strain.

Another structural feature which exhibits a large strain is the interpolyhedral O–O distance. The smallest O–O interpolyhedral distance at ambient pressure is 3.4 Å. This value decreases to approximately 2.6 Å at 20 GPa. In naturally occurring silicates, the smallest known interpolyhedral distance is 2.75 Å which occurs in Be_2SiO_4. This suggests that the α-quartz structure may be becoming unstable at pressures greater than about 20 GPa as the minimum interpolyhedral distance approaches the smallest known value. Moreover, the behavior of this distance with pressure exhibits non-linear behavior above 15 GPa.

While the Si–O–Si angles and the interpolyhedral O–O distances exhibit non-linearities with pressure, these do not provide a quantitative measure for mechanical instability. However, with first principles methods, it is possible to calculate the elastic constants directly as a function of pressure. Under initial hydrostatic pressure, the elastic constants $c_{\alpha\beta\gamma\delta}$ are related to the energy variation ΔE to second order in the strains $\epsilon_{\alpha\beta\gamma\delta}$, through [32]

$$\frac{\Delta E}{V_0} = -p\frac{\Delta V}{V_0} + \frac{1}{2}\sum_{\alpha,\beta,\gamma,\delta} c_{\alpha\beta\gamma\delta}\,\epsilon_{\alpha\beta}\,\epsilon_{\gamma\delta} \quad (4)$$

where $\Delta V = V - V_0$. p, V are the initial pressure and volume respectively.

$$\Delta V = \sum_{\alpha\alpha}\epsilon_{\alpha\alpha} + \frac{1}{4}\sum_{\alpha\beta\gamma\delta}[2\delta_{\alpha\beta}\delta_{\gamma\delta} - \delta_{\alpha\delta}\delta_{\beta\gamma} - \delta_{\alpha\gamma}\delta_{\beta\delta}]\epsilon_{\alpha\beta}\,\epsilon_{\gamma\delta}$$

is the volume change to the second order in the strain. For α-quartz, it is possible using symmetry to reduce the number of independent elastic constants to six [33]: c_{11}, c_{12}, c_{13}, c_{14}, c_{33}, c_{44} where $1 = xx$, $2 = yy$, $3 = zz$, $4 = yz$. The elastic energy must be positive. This condition imposes the following constraints, the Born criteria:

$$c_{11} - |c_{12}| > 0 \quad (5)$$

$$(c_{11} + c_{12})c_{33} - 2c_{13}^2 > 0 \quad (6)$$

$$(c_{11} - c_{12})c_{44} - 2c_{14}^2 > 0 \quad (7)$$

for the crystal to be mechanically stable. The first criterion (5) insures that the squared velocity of a transverse elastic wave in the plane perpendicular to the c-axis is positive. The second criterion (6) corresponds to positive bulk modulus. The third criterion (7) corresponds to shear-waves in planes including the c-axis. We have evaluated [34] the elastic constants as a function of pressure and find that the first two criteria are met at ambient conditions and for pressures well above the amorphization transformation. However, the third criterion is violated at a pressure of around 30 GPa which is consistent with the collapse of the crystalline phase observed experimentally at that pressure.

The microscopic nature of this instability appears to be associated with the formation of the b.c.c. anion packing at high pressure. Our analysis suggests that the instability is intimately related to the coordination change of the silicon cation from a four-fold to a six-fold site. In the picture suggested by first principles calculations, as pressure is applied to the α-quartz structure a mechanical strain builds up. This strain is confirmed by the small Si–O–Si bond angle and the interpolyhedral O–O distances. The non-linearity of the angle and distance changes with pressure above about 15 GPa reinforce this picture of large mechanical strains near the amorphization transformation. We confirm that near this transformation the α-quartz structure assumes a b.c.c. packing of the anions. Moreover, this b.c.c. packing is accompanied by a mechanical instability in which one of the Born criteria is violated. In this unstable arrangement, we envision silicon cations diffusing from tetrahedral to octahedral sites. At high pressures, the silicon cations occupy primarily octahedral sites, and a rutile-like *i.e.* stishovite, structure occurs.

5. Conclusions

We have illustrated in this paper how first principles total energy calculations can be used to examine structural trends for crystalline silica. These approaches are particularly powerful as they require no experimental input, yet they yield accurate structural information. For example, in the case of α-quartz the only input into the calculations are the atomic numbers of silicon and oxygen, and the crystal symmetry. With this input one is able to compute accurately the ambient structural parameters, the cohesive energy, compressibility, *etc.*, and the behavior of quartz under pressure.

We focused on the behavior of crystalline silica under pressure in terms of phase stability, and on the stability of a given phase, α-quartz, with respect to amorphization under pressure. We found that our pseudopotential calculations reproduce accurately the known phases of crystalline silica. In particular, we find that α-quartz is the most stable form of silica at ambient pressure. At elevated pressure, we find that the stishovite structure is more stable. In this structure, the silicon cations change from being a four-fold coordinated species to a six-fold coordinated species. This increased coordination is accompanied by a large change in the density, although the total electronic energy remains nearly equal to that of α-quartz. If the pressure is further increased, we find that the stishovite structure becomes unstable when compared with the $Pa\bar{3}$ structure. The $Pa\bar{3}$ structure is a distortion of the fluorite structure; the silicon cation becomes eight-fold coordinated. We find that silica will never be stable within the ideal fluorite structure.

We also examined the behavior of α-quartz as a function of pressure. This crystal is known to amorphize near 30 GPa. At even higher pressures (near 60 GPa), this material appears to recrystallize in the rutile structure. Unphysically small bond angles and O–O interpolyhedral distances in α-quartz indicate the material may become mechanically unstable above about 15 GPa. We confirmed this by computing the elastic constants of α-quartz. We find that above about 30 GPa, one of the Born criteria for mechanical stability is violated by the quartz elastic constants. We also find that if the α-quartz structure were subjected to higher pressures, the oxygen anions would form a b.c.c. array. This arrangement would promote diffusion of the silicon cations from four-fold to six-fold sites, and could account for the ease of rutile formation at high pressures.

As this work illustrates, first principles calculations can be valuable tools for exploring the structure of solids. Although it is not generally possible to examine an entire family of structures with varying stoichiometry, it is possible to examine the details of a given structure

and obtain a detailed picture of the chemical bonding force within that structure.

Acknowledgments

We would like to acknowledge support for this work by the US Department of Energy of the Office of Basic Energy Sciences (Division of Materials Research) under Grant No. DE-FG02-89ER45391. We would also like to acknowledge computational support from the Minnesota Supercomputer Institute.

References

1 M. L. Cohen, in J. R. Chelikowsky and A. Franciosi (eds.), *Electronic Materials: A New Age in Materials Science,* Springer Solid State Science Vol. 95, Springer, Berlin, 1991, p. 57.
2 K. J. Chang, M. M. Dracorona, M. L. Cohen, J. M. Mignot, G. Chouteau and G. Martinez, *Phys. Rev. Lett., 54* (1985) 2375.
3 N. Troullier and J. L. Martins, *Phys. Rev. B, 43* (1991) 1993.
4 P. Ballone and W. Andreoni, *Phys. Rev. Lett., 60* (1988) 217.
5 N. Binggeli, J. L. Martins and J. R. Chelikowsky, *Phys. Rev. Lett., 68* (1992) 2956.
6 P. Villars, J. C. Phillips and H. S. Chen, *Phys. Rev. Lett., 57* (1986) 3085.
7 J. R. Chelikowsky and M. L. Cohen, Ab initio pseudopotentials for semiconductors, *Handbook on Semiconductors,* 2nd edn., in press.
8 W. Kohn and L. Sham, *Phys. Rev. A, 140* (1965) 1133.
9 P. Hohenberg and W. Kohn, *Phys. Rev. B, 136* (1964) 864.
10 S. Lundqvist and N. H. March, *Theory of the Inhomogeneous Electron Gas,* Plenum, New York, 1983, and references cited therein.
11 J. L. Martins and M. L. Cohen, *Phys. Rev. B, 37* (1988) 6134.
12 J. L. Martins, N. Troullier and D. S. -H. Wei, *Phys. Rev. B, 43* (1991) 2213.
13 J. Ihm, A. Zunger and M. L. Cohen, *J. Phys. C, 12* (1979) 4409.
14 W. G. Wyckoff, *Crystal Structures,* Interscience, New York, 1974, 4th edn.
15 J. R. Chelikowsky, H. E. King, Jr., N. Troullier, J. L. Martins and J. Glinnemann, *Phys. Rev. Lett., 65* (1990) 3309; *Phys. Rev. B, 43* (1991) 489.
16 N. Binggeli, N. Troullier, J. L. Martins and J. R. Chelikowsky, *Phys. Rev. B, 44* (1991) 4771.
17 N. Keskar, N. Troullier, J. L. Martins and J. R. Chelikowsky, *Phys. Rev. B, 44* (1991) 4081.
18 N. Keskar and J. R. Chelikowsky, *Phys. Rev. B, 46* (1992) 1.
19 F. Birch, *J. Geophys. Res., 57* (1952) 227.
20 R. E. Cohen, *Am. Mineral., 76* (1991) 733.
21 L. Levien, C. T. Prewitt and D. J. Weidner, *Am. Mineral., 65* (1980) 920.
22 J. D. Bass, R. C. Libermann, D. J. Weidner and S. J. Finch, *Phys. Earth Planet. Interiors, 25* (1981) 140.
23 V. G. Zubov and M. M. Firsova, *Kristallographia, 1* (1956) 546.
24 N. L. Ross, J. Shu, R. M. Hazen and T. Gasparik, *Am. Mineral., 75* (1990) 739.
25 M. Sugiyama, S. Endo and K. Koto, *Mineral. J., 13* (1987) 455.
26 R. M. Hazen, L. W. Finger, R. J. Hemley and H. K. Mao, *Solid State Commun., 72* (1989) 507.
27 R. J. Hemley, A. P. Jepcoat, H. K. Mao, L. C. Ming and M. H. Manghnani, *Nature, 334* (1988) 52.
28 Y. Tsuchida and T. Yagi, *Nature, 347* (1990) 267.
29 H. Sowa, *Z. Kristallogr., 184* (1988) 257.
30 N. Binggeli and J. R. Chelikowsky, *Nature, 353* (1991) 344.
31 Y. S. Tse and D. D. Klug, *Phys. Rev. Lett., 67* (1991) 3559.
32 T. H. K. Barron and M. L. Klein, *Proc. Phys. Soc., 85* (1965) 523.
33 F. I. Fedorov, *Theory of Elastic Waves in Crystals,* Plenum, New York, 1968.
34 N. Binggeli and J. R. Chelikowsky, *Phys. Rev. Lett., 69* (1992) 2220.